

QSAR study and molecular docking of benzimidazole derivatives inhibitors of p38 kinase

N. Naceiri Mrabti ^{*1}, K. Dguigui^{1*}, H. Hadni¹, M. Elhallaoui²

¹ Engineering Materials, Modeling and Environmental Laboratory, Faculty of Science, University Sidi Mohammed Ben Abdellah, Dhar Mehraz, B.P. 1796, Atlas, Fes, Morocco

² Department of Chemistry, Faculty of Science, University Sidi Mohammed Ben Abdellah, Dhar Mehraz, B.P. 1796, Atlas, Fes, Morocco

* Corresponding author:

nidal.naceirimrabti@usmba.ac.ma

Received 17 Jun 2017,

Revised 25 May 2018,

Accepted 27 May 2018

Abstract

3D-QSAR and Molecular Docking methods were performed on a set of 42 benzimidazolone derivatives considered as inhibitors of the MAPK (Mitogen Activated Protein Kinases) that play critical roles in cell signaling and gene expression. IC₅₀ of 42 compounds is quantitatively modeled by using Multiple Linear Regression (MLR), and Neuronal Networks (NN). The proposed QSAR model has provided statistically significant results ($R_{MLR} = 0.90$; $R_{NN} = 0.92$ and $R_{CV} = 0.91$), It is validated by leave-one-out method. The general interaction mode of molecules to the P38 Kinases binding sites was explored by using Molecular Docking techniques. In this paper we are focused on the most active molecules of our set, compound 34, and has been compared by the 4-[5-(4-fluoro-phenyl)-2-(4-methanesulfinyl-phenyl)-3H-imidazol-4-yl]-pyridine that is highly interactive with the site P38 alpha Mitogen Activated Protein kinases.

Keywords: Benzimidazole derivatives; Quantitative structure–activity relationship (QSAR) Multiple Linear Regression (MLR); Neural network (NN); Molecular docking

1. Introduction

P38 is a member of the Mitogen Activated Protein Kinase (MAPK) family, it is a key enzyme involved in many cellular regulations, including signaling pathways, pain and inflammation [1- 4]. There are four members of the p38MAPK family (p38 α , p38 β , p38 γ and p38 δ). Among all the isoforms p38 MAPK, p38 is the best characterized and is expressed in most cell types [5]. Mitogen activated protein kinases are member of intracellular kinases that play critical roles in cell signaling and gene expression. The p38 MAPK cascade is stimulated by various proinflammatory cytokines, such as TNF-alpha and activation of the P38 MAPK signaling culminates in increased expression of proinflammatory molecules like TNFA-alpha, IL-6, IL-8, and metalloproteinases [6]. The activation of P38 is responsible for the formation of inflammatory cytokines such as TNF-alpha and interleukin IL-1 β , accordingly, the P38 MAPK inhibitor acts as a therapeutic drug for the treatment of chronic inflammatory diseases such as Rheumatic Arthritis (RA) by regulating the secretion of cytokines [7]. In the present paper, we describe a new 3D-QSAR model for benzimidazole compounds known as P38 MAPK inhibitors, [8] this QSAR is a methodology to use the correlation between properties chemical structures and their activity profiles ,also, it uses for predicted the biological activity of non synthesized compounds structurally [9]. In this 3D-QSAR we are used the Multiple Linear Regression (MLR), and Neuronal Networks (NN) and Docking Molecular.

2. Material & methods

2.1. Data set

For the present molecular modeling study, a set of 42 benzimidazole was obtained from published literature (Mark, A and al.,) [9], this serie of benzimidazolone were identified as a new class of anti-inflammatory targeted to inhibit P38 kinase and thereby inhibiting the release of proinflammatory cytokine. In this work, the IC₅₀ values were converted to the corresponding log (IC₅₀). All the compounds and associated inhibitory activity are listed in **Table 1**.

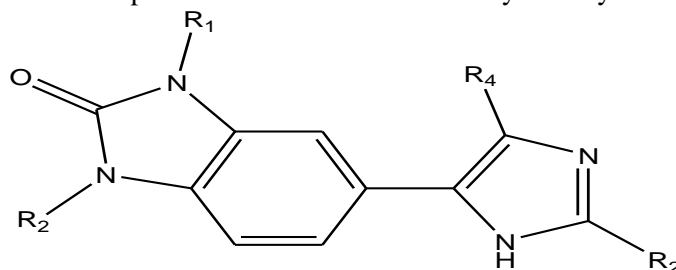
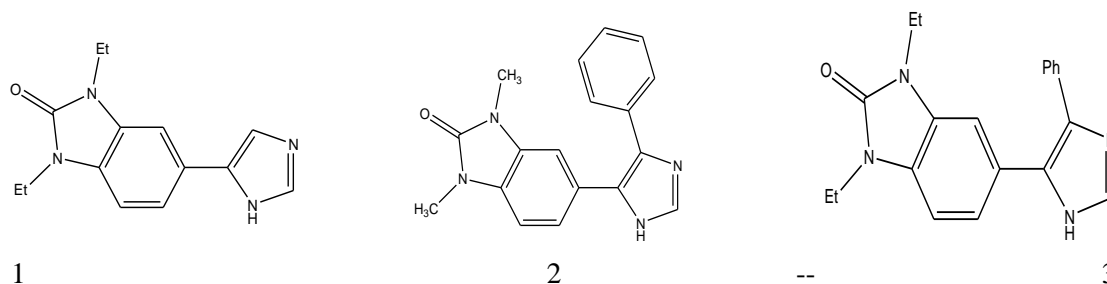
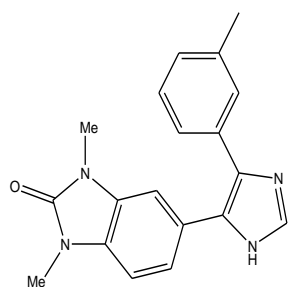


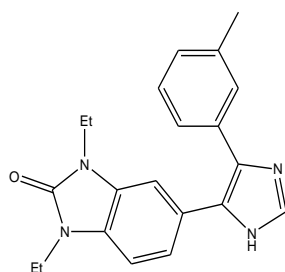
Fig1: Molecule of benzimidazole derivatives

Table 1: List of benzimidazole derivatives Structures with their observed activities

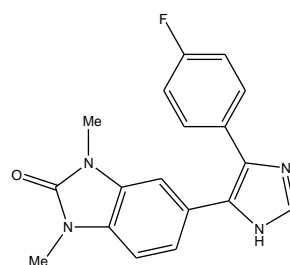




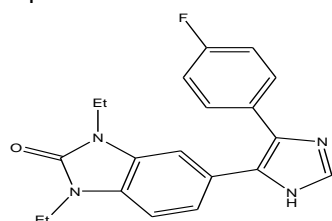
4



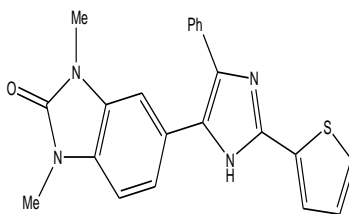
5



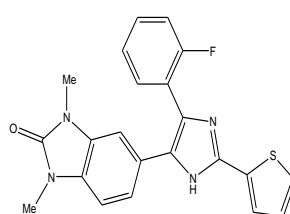
6



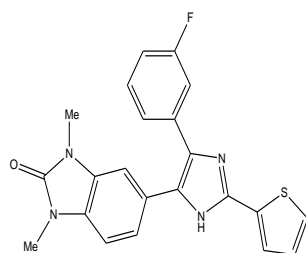
7



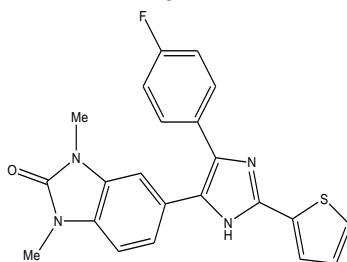
8



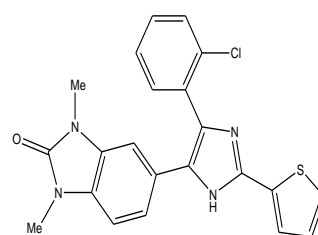
9



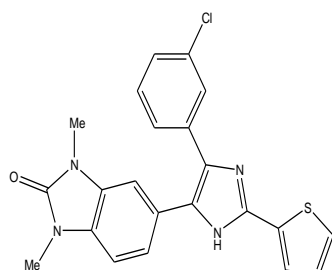
10



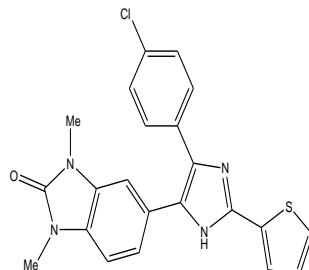
11



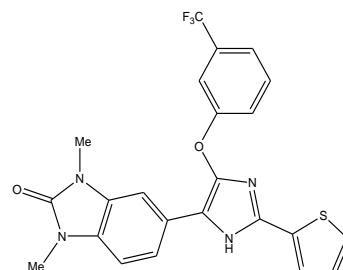
12



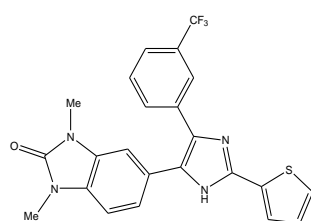
13



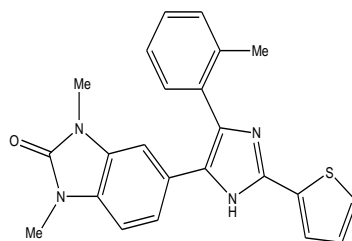
14



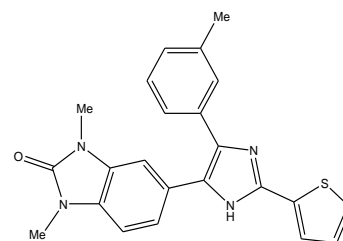
15



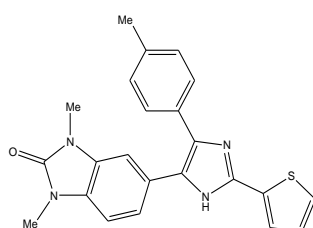
16



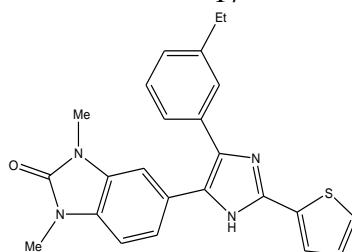
17



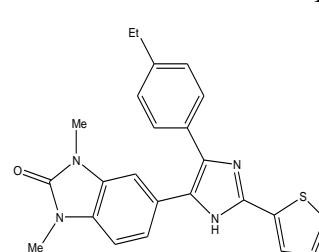
18



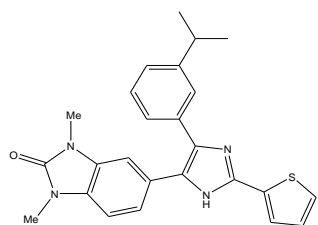
19



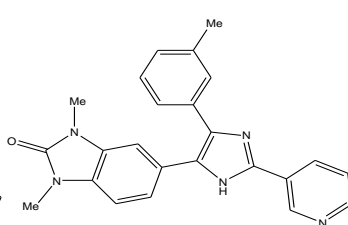
20



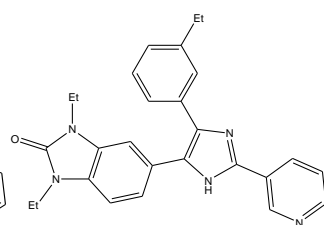
21



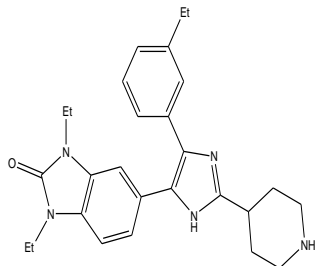
22



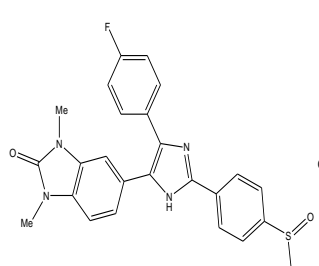
23



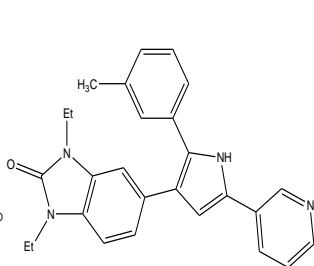
24



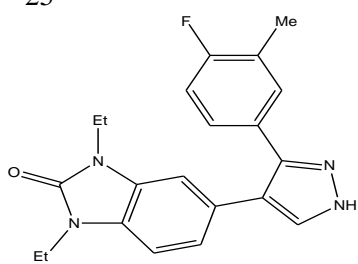
25



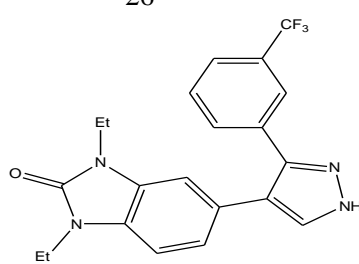
26



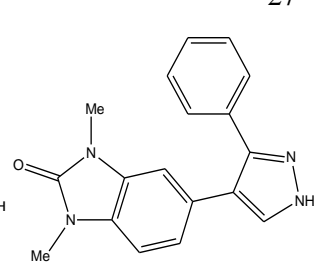
27



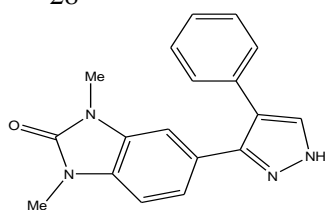
28



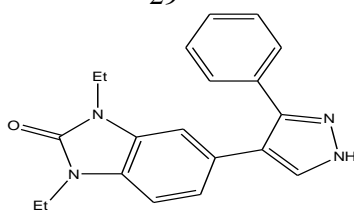
29



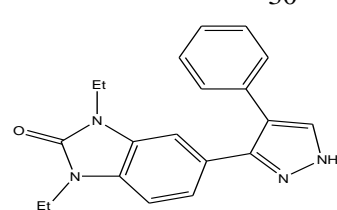
30



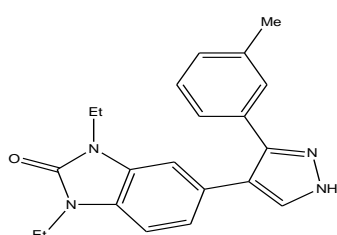
31



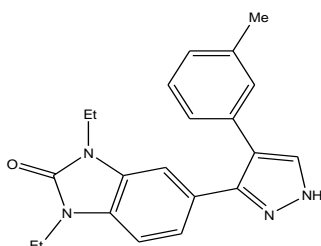
32



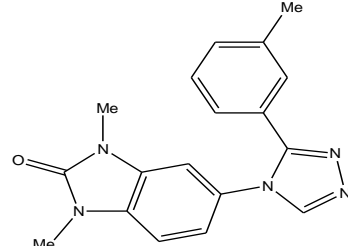
33



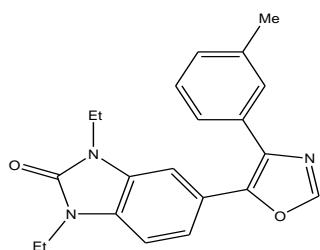
34



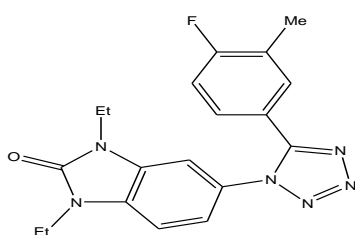
35



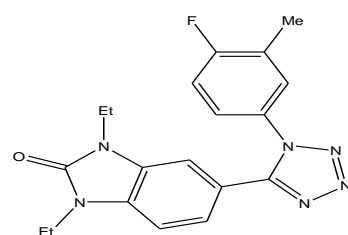
36



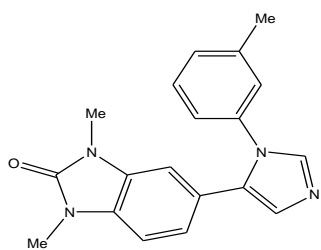
37



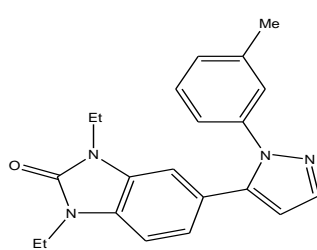
38



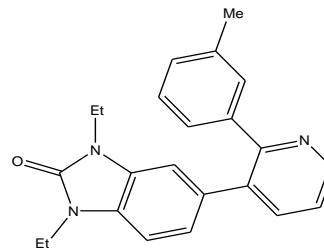
39



40



41



42

2.2. Descriptor generation

The Molecular descriptors are obtained by ChemDraw and Gaussian 03:

• Calculation of steric, thermodynamic, and topologic chemical descriptors:

All of the molecular structures of the compounds were initially optimized geometrically using the MM2 method (minimize energy), and the descriptors Steric, Thermodynamic and Topological are carried by using Chemdraw 03.

The descriptors taken from this software are : Radius (Rad) ,Molecular Weight(MW), Cluster Count (ClsC) ,Wiener Index (Windx) ,Parachor (Par), Balban Index (Blndx),Molecular Topological Index (TIndx), lypophilie (LogP) Molecular Refraction(RM),Henry's law constant (H) ,Heat of Formation (HF) ,VDW Energy (E_{VDW}) and Torsion Energy(Et).

• Calculation of quantum chemical descriptors:

The molecular structures of all compounds were drawn using GaussView [9] and the molecular descriptors quantum were calculated by Gaussian 03[10].The geometry optimization and energy calculations of benzimidazole derivatives were carried out using DFT (B3LYP) methods with 6-31G* basis sets, [11-13]. The descriptors obtained for our model in this work include: Total energy (E_{Total}), highest occupied molecular orbital energy (E_{HOMO}), lowest unoccupied molecular orbital energy (E_{LUMO}), total dipole moment (μ) of the molecule, the electron affinity (EA) ,the ionization potential (IP),The energy gap ($E_{HOMO}-E_{LUMO}$), Mulliken Electronegativity (χ),Hardness (η),Electrophilicity (ω),Softness (S) and Electrophilicity index (ω_i). The knowledge that:

$EA = -E_{LUMO}$, $IP = -E_{HOMO}$, $\chi = (E_{LUMO} + E_{HOMO})/2$, $\eta = (E_{LUMO} - E_{HOMO})/2$, $\omega = (E_{LUMO} + E_{HOMO}/2)^2/2$, $S = 1/2 \eta$ and $\omega_i = \mu^2/2 \eta$.

2.3. Multiple Linear Regression:

The QSAR model is developed using the standard method for multivariate data analysis, the multiple linear regression (MLR). It's also called as ordinary least squares regression (OLS). So, MLR estimates the values of the regression coefficients by applying least squares curve fitting method [14].

$$Y_{MLR} = a_0 + \sum_{i=1}^n a_i \times C_i$$

Or, Y_{MLR} : dependent variable; a_0 : regression constant or intercept; a_i : regression coefficient ; C_i : independent variable; The Multiple Linear Regression model (MLR) has served also to select the descriptors used as the input parameters for a back propagation network (NN).

2.4. Neural Network:

Neural network (NN) establishes nonlinear correlation between molecular and/or structural descriptors of chemicals and their biological activities. An artificial neural network is a connected set of mathematical functions that processes each descriptor through three layers of neurons (input, hidden and output layers) Fig. 1 Some authors [15] have proposed a parameter p , leading to determine the number of hidden neurons, which plays a major role in determining the best ANN architecture. It's defined as follows:

$\rho = (\text{Number of data points in the training set}) / (\text{Sum of the number of connections in the NN})$

Therefore, in order to avoid overfitting and underfitting, it's recommended to take into account the ρ value; $1.8 < \rho < 2.3$ [16].

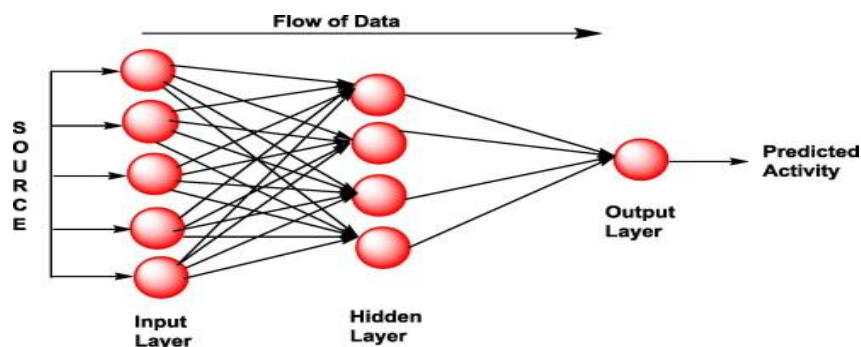


Fig. 2.A simplified sketch for the artificial neural network structure.

2.3. Cross Validation

Cross validation was carried out by the Leave-One-Out (LOO) procedure. [17-19], and the correlation coefficient R_{cv} (Q^2) was calculated with following equation: $R_{cv} = Q^2 = 1 - \sum (Y_{pred} - Y_{exp})^2 / \sum (Y_{exp} - Y_{mean})^2$

Where Y_{pred} , Y_{exp} and Y_{mean} are the values for the predicted activity, experimental activity and mean activity, respectively.

2.4. Docking molecular

To gain better understanding on the potency of the compounds, we proceeded to examine the interaction of the benzimidazole derivatives with P38. The molecular docking was performed by inserting of compound 34 into the site P38 alpha kinase. The docking is applied in AutoDock Tools-1.5.6 and the visualization of results is fact in Discovery Studio 3.5. [20],

✓ Preparation protein

Three-dimensional structure information on the target protein was taken from the PDB (<http://www.rcsb.org> / code: 1A9U). Processing of the protein included the deletion of the ligand, this ligand co-crystallized with active site allowed to know the residues which are contact with this ligand and determine the active site and the main residues included in this activation, finally, the removal solvent molecules and addition the hydrogen atoms using AutoDockTools-1.5.6 software [21], Fig3.

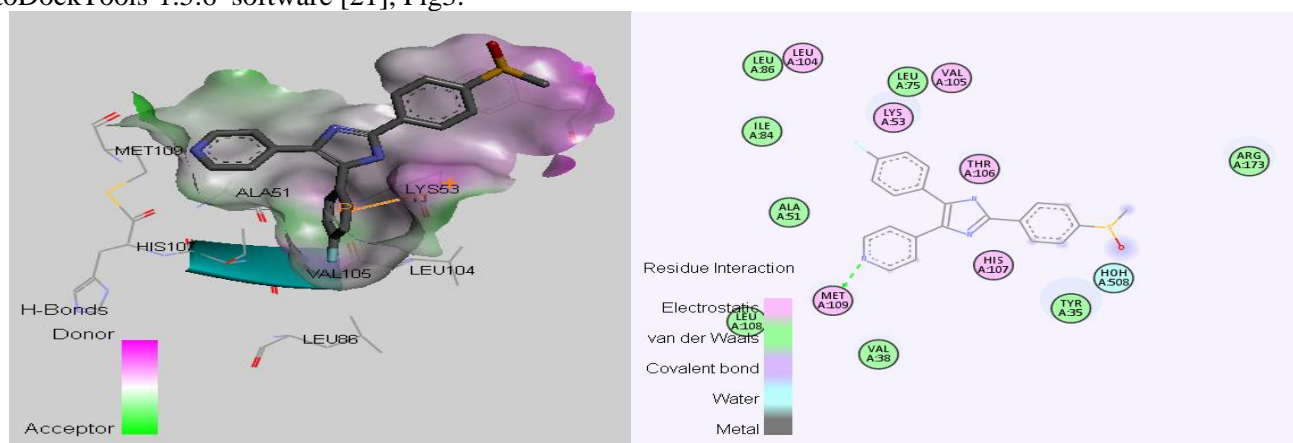


Fig3: Left image, shows the three dimension co-crystallized ligand in the active site P38alpha. Right, Met109, Thr106, Val105, Lys53Leu104, Val38, Tyr35Leu75, Ile84, Leu86, Ala51, Leu108and Arg173 residues are presented the active site main.

The molecular structure and chemical formula of co-crystallized ligand (4-[5-(4-fluoro-phenyl)-2-(4-methanesulfinyl-phenyl)-3H-imidazol-4-yl]-pyridine) with the protein is shown in the following figure.

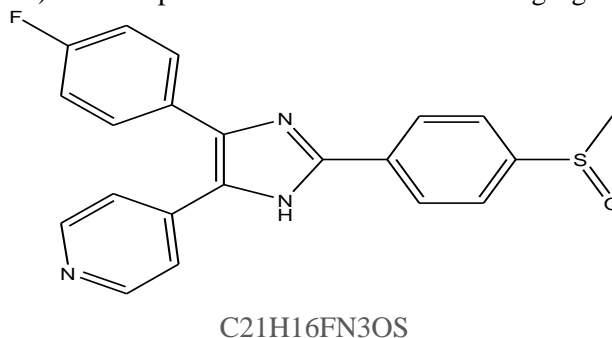


Fig 4: Molecular structure and chemical formula of Co-crystallized ligand:

✓ Preparation of ligand :

The Compound 34 (Fig.4) is optimized at B3LYP / 6-31G (d, p) (# opt B3LYP / 6-31G geom= connectivity) to obtain the most stable form, the file obtained is saved under extension (ligand.pdb)

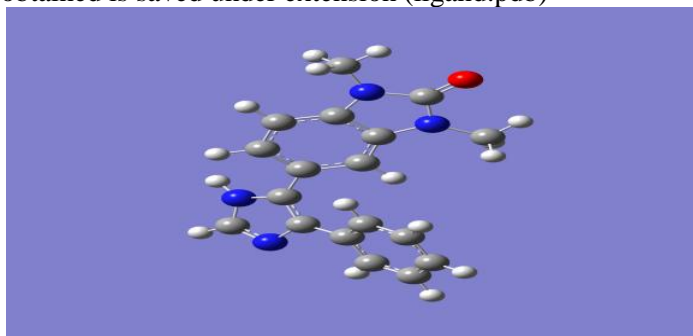


Fig5: form geometry obtained by gauss 03

✓ Docking by using AutoDock Tools-1.5.6 software:

To investigate the intermolecular interactions between the ligand and the target protein, the docking program AutoDock was used. It calculates the intermolecular “energies” by adding up all intermolecular interactions (Van-Der-Waals, electrostatic) that occur between ligand and protein. The 3D structures of ligand molecule were saved in PDB format with the aid of the program chembio3D [23]. The PDB file was further modified by using the ADT package (version 1.5.6) so that the charges of the no polar hydrogen atoms would be assigned to the atom to which the hydrogen is attached. The resulting file was saved as PDBQT file. In this docking a grid box size of 40, 40, 40, pointing in x, y and z directions was built, the maps were centered on the compound 34 in the catalytic site of the protein. A grid spacing of 1 Å and a distances-dependent function of the dielectric constant were used for the calculation of the energetic map. Finally, the result docking are saved on nine complexes, the complex which has been selected is less energetic.

3. Results and Discussions

Strong activity was observed when inhibitors possess a variety of substituted heterocyclic including imidazoles, triazoles, oxazole, pyrroles and pyridines by assembly with the benzimidazole.

The selected descriptors values, and predicted activities values obtained by MLR, ANN and CV methods, are summarized in table 2.

Table 2: Values of the selected descriptors, and the observed/predicted IC_{50} values

Compounds	Log P ^b	E ^a _{HUMO}	E ^b _{VDW}	Dip/Dip ^b	LogIC _{50exp}	IC ₅₀ (Theo)		
						LogIC _{50RML}	LogIC _{50RML}	Log IC _{50RML}
1	4,3770	-1,1587	9,5258	-1,5447	0,0414	-0,1035	0,0415	0,0957
2	4,4220	-1,3244	16,9860	-16,5038	-0,5376	-0,5407	-0,6174	-0,3023
3	4,1460	-1,0340	18,3737	-16,1789	-0,8539	-0,3586	-0,4267	-0,4677
4	2,7570	-0,8139	17,5621	-16,5396	-1,0000	-1,0751	-1,000	-1,054
5	2,2390	-0,7910	18,9899	-16,2145	-1,3010	-1,1041	-1,3934	-1,4566
6	3,2440	-0,9603	16,8852	-16,3354	-0,8539	-0,9647	-0,8539	-0,9829
7	2,9150	-0,9519	18,2696	-16,0038	-1,0000	-0,9137	-1,1741	-1,1704
8	4,1160	-1,3369	18,6138	-15,0320	-0,5850	-0,3534	-0,5323	-0,3809
9	4,2740	-1,3393	18,3656	-13,9107	-0,4318	-0,2097	-0,5717	-0,3235
10	4,2740	-1,4305	18,5490	-14,9486	-0,4089	-0,3138	-0,4917	-0,3584
11	4,2740	-1,4275	18,5074	-14,8284	-0,5686	-0,3072	-0,5067	-0,3477
12	4,6740	-1,3540	19,0626	-14,1915	-0,2676	0,0391	-0,2368	-0,1011
13	2,9510	-1,4596	19,2274	-14,9672	-0,4202	-0,8730	-0,643	-0,9735
14	4,6740	-1,4681	19,0557	-14,8282	-0,1675	-0,0617	-0,2281	-0,1072
15	5,1910	-1,6381	26,5093	-14,0697	1,1987	1,1340	1,1238	1,2271
16	4,2390	-1,5154	19,2732	-14,9209	0,1761	-0,2682	0,0935	-0,3392
17	4,6030	-1,3549	23,7501	-15,2127	0,7924	0,5072	0,8606	0,742
18	4,6030	-1,3198	19,1894	-15,0675	-0,8539	-0,0444	-0,1952	-0,2147
19	4,6030	-1,3176	19,2491	-15,0708	0,2553	-0,0363	-0,1849	-0,2258
20	3,9880	-1,3238	20,1937	-15,0687	-0,3010	-0,2128	-0,2615	-0,2083
21	5,0200	-1,3146	24,7922	-15,0709	0,9031	0,8665	1,0294	0,9959
22	5,3500	-0,0876	27,1800	-15,0684	1,5185	1,7881	1,5191	1,1317
23	3,2840	-1,3257	19,5625	-16,3955	-0,6990	-0,7491	-0,6884	-0,6738
24	2,5680	-1,3652	19,1093	-16,0709	-1,1549	-1,1345	-1,1551	-1,1095
25	2,4460	-0,7121	19,3846	-15,9639	-1,1549	-0,9030	-1,1173	-0,9261
26	4,6740	-1,0182	22,0417	-18,2802	0,6021	0,1761	0,3514	0,5142
27	4,4020	-0,9992	21,0172	-15,3046	0,0414	0,1903	0,0635	0,218
28	2,0800	-0,6123	19,2801	-15,8027	-1,5229	-1,0392	-1,4016	-0,919
29	2,3680	-1,1334	19,5684	-15,4029	-1,2218	-1,0250	-1,3122	-1,2189
30	2,8250	-0,5206	17,1155	-15,4230	-0,6990	-0,8888	-0,6917	-0,9834
31	2,8250	-0,5206	17,0850	-15,5434	0,3979	-0,9035	0,3979	-0,7228
32	3,5010	-0,5472	18,5053	-15,0954	-0,6990	-0,3701	-0,6049	-0,6994
33	3,5010	-0,5048	18,4692	-15,2199	-0,1675	-0,3699	-0,2116	-0,2502
34	1,5700	-1,6836	19,2049	-15,3809	-2,0458	-1,6573	-1,9338	-1,5998
35	3,9880	-0,4667	19,0737	-15,2763	-0,1367	-0,0512	-0,1062	-0,048
36	5,0200	-1,0251	24,8349	-16,6766	1,0969	0,8367	1,0866	0,9664
37	3,3160	-1,2754	20,2502	-14,8896	-0,0969	-0,4927	-0,1253	-0,1891
38	3,6870	-1,6738	20,9690	-15,6039	0,0414	-0,4380	0,1602	-0,4344
39	3,6870	-0,4931	21,0338	-15,8115	0,0414	-0,0047	-0,0826	-0,077
40	5,0370	-0,7328	25,7087	-16,7184	1,1584	1,0616	1,1482	1,1044
41	3,8440	-0,8163	20,7443	-15,3304	-0,1612	-0,0447	-0,1459	-0,0192
42	4,5510	-0,9227	20,2413	-15,1168	0,0414	0,2088	0,0142	0,1327

a: using Gaussian03W software, b: using chembio3D software.

3.1. Multiple Linear Regression

we have correlate all variables for to eliminate the strongly correlated variables, then we did the multiple linear regression between the remains of the variables (independent) and the values of the activities (dependent). In this study, we used the method of stepwise regression which consists to selected a reduced number of descriptors. The QSAR model built using multiple linear regression (MLR) method is represented by the following equation:

$$\text{Log IC}_{50} = -2,829 + 0,478 \text{ Log P} + 0,376 E_{\text{HUMO}} + 0,127 E_{\text{VDW}} + 0,090 \text{ Dip/Dip} \quad (\text{Eq (1)})$$

$$N=42 \quad R_{\text{MLR}}=0.90 \quad R^2_{\text{MLR}}=0.80 \quad \text{SE}=0,368 \quad F=37,325$$

Where N is the number of compounds included in the model, r is the correlation coefficient, R^2 is the Squared Multiple, SEE is the Standard Error of Estimate and F is the Fisher F-statistic. The correlation coefficient between Log IC₅₀exp and LogIC₅₀MLR is $R=0,90$ which means that the selected descriptors are able to form good QSAR-model. The contribution of descriptors to this model is illustrated in figure 6.

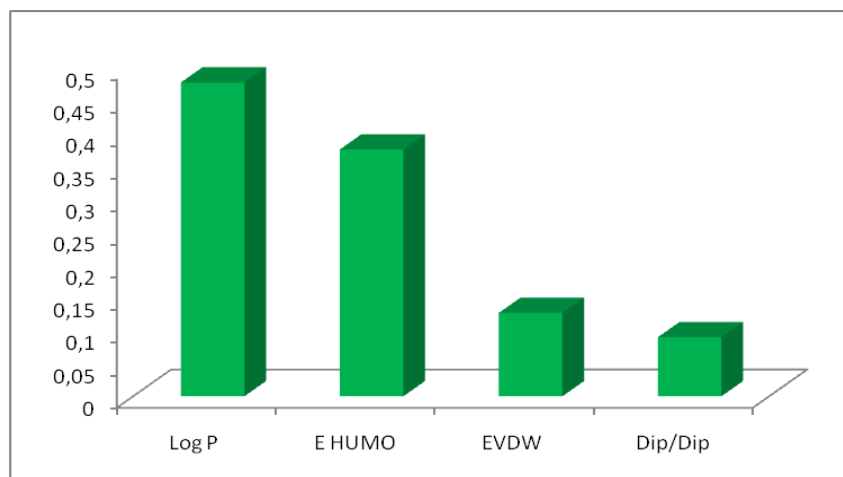


Fig6: Contribution of descriptors to the QSAR model

Figure 6 indicates that the relative importance of the descriptors varied in the following order: LogP > E_{HUMO} > EVDW > Dip/Dip. So, we can notice that LogP and E_{HUMO} are the most important descriptors in the establishment of the QSAR model of benzimidazole derivatives, which means that the activity is related to hydrophobic and electronic effects. The graphical correlation of observed and predicted IC₅₀ by MLR is recorded in figure 7.

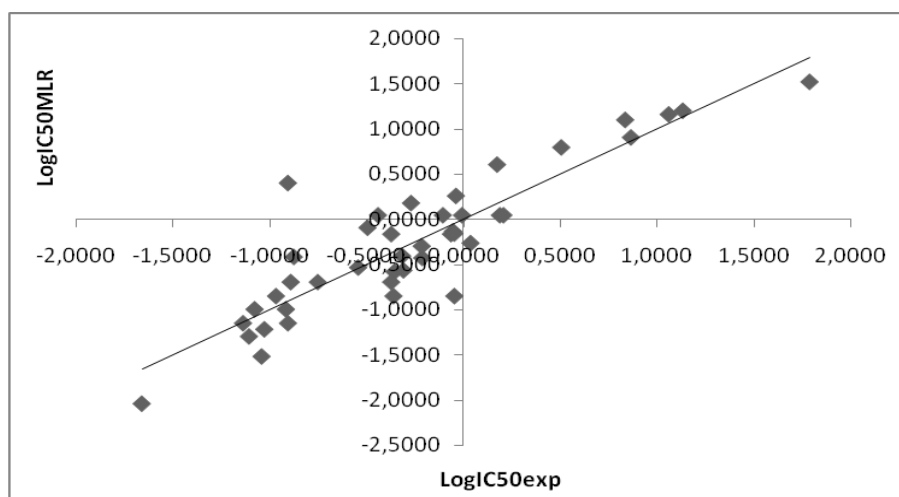


Fig7: Predicted activities by MLR related to experimental Values of IC₅₀

3.2. Neural Networks

In order to increase the probability of good characterization of studied compounds, the artificial neural network (ANN) is used to generate predictive model of quantitative structure-activity relationships (QSAR) between a set of molecular descriptors obtained by MLR method, and IC_{50} values observed. The **figure 8** shown a good correlation between observed IC_{50} values and ANN predicted.

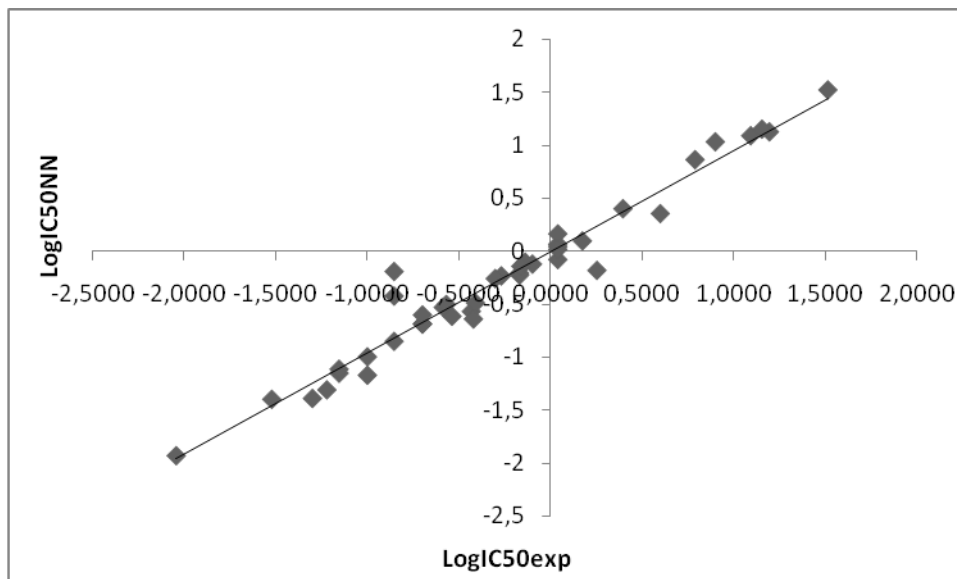


Fig8: Predicted activities by ANN related to experimental Values of IC_{50}

$n = 42$, $R = 0.92$, $R^2 = 0.84$, $SD = 0.1$

3.3. Cross-Validation

The QSAR model proposed to predict the activity of new compounds should be validated before its use. In this paper we validated our model with cross validation method. The good results obtained

($N = 42$, $R_{cv} = 0.91$, $R^2_{cv} = 0.82$) show that the predictive power of this model is very significant. So, the most important result of this investigation is that biological activity could be predicted using QSAR methods, and that the selected descriptors are pertinent. The graphical correlation of observed and predicted IC_{50} by CV is recorded in **figure9**.

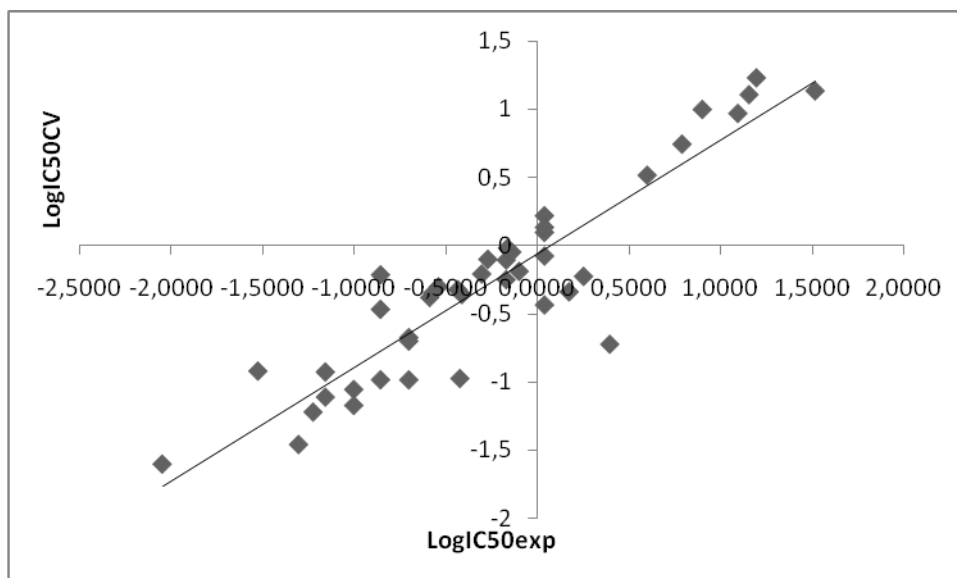


Fig9: Predicted activities by CV related to experimental Values of IC_{50}

3.4. Molecular docking studies of inhibitors of p38 kinase and the binding conformation:

Molecular docking has contributed important insights into drug discovery for many years. However, docking procedures aim to identify correct positions of ligands in the binding pocket of a protein and to predict the affinity between the ligand and the protein. In this study the Docking molecular is carried to explore the probable bindings of inhibitor (compound 34) with the receptor and to examine significant interactions with the protein. The binding model of compound 34 and P38 alpha was depicted in **Fig 4**, and the enzyme surface model was shown in **Fig 5**. This revealed that the molecule is well filled in the active pocket.

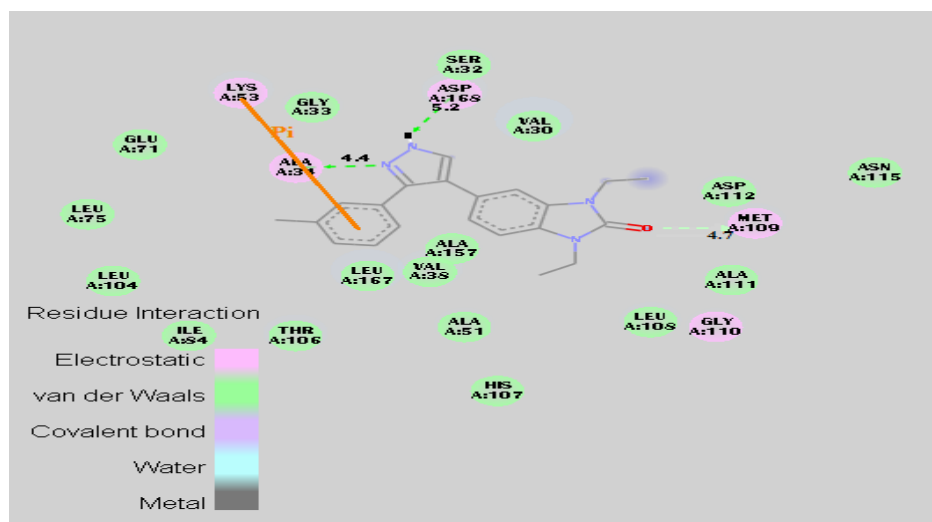
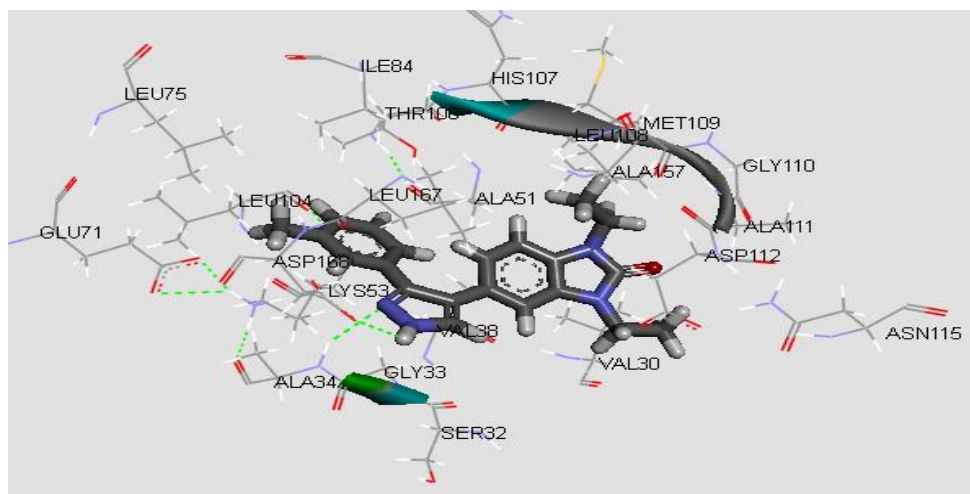


Fig 10 : Binding mode of compound 34 with P38 alpha. H-bonding interactions are shown in dotted lines. This figure was made using Discovery Studio 3.5



Meanwhile, the receptor surface model showed in **Fig. 5** revealed that this inhibitor (compound 34) was integrated into the active site of P38 alpha kinase. This molecular docking result, suggested that compound 34 is a potential inhibitor of P38 alpha.

In the binding mode, compound 34 is nicely bound to P38alpha via two hydrogen bonds. The hydrogen atom on the pyrazol ring with the oxygen atom on the main chain of Ala₃₄ (distance = 4.40 Å) and the hydrogen atom of compound with the oxygen atom on the hydroxyl of Asp₁₆₈ (distance = 5.2 Å).

There are some Van Der Waals contacts between compound and the following residues Ala₁₁₁, Ala₅₁, Ala₁₅₇, His₁₀₇, Ile₇₅, Ile₈₄, Val₃₀, Val₃₈, Leu₇₅, Leu₁₀₈, Leu₁₀₄, Leu₁₆₇, Ser₃₂, Gly₃₃, Glu₇₁ and Thr₁₀₆.

Finally, compared with co-crystal used in this work, we found that the main residue introduced into the activation of protein such as: Met₁₀₉ residue, is the same found in the interaction with the compound 34, these results, confirm that this compound is very inhibitory to P38alpha protein.

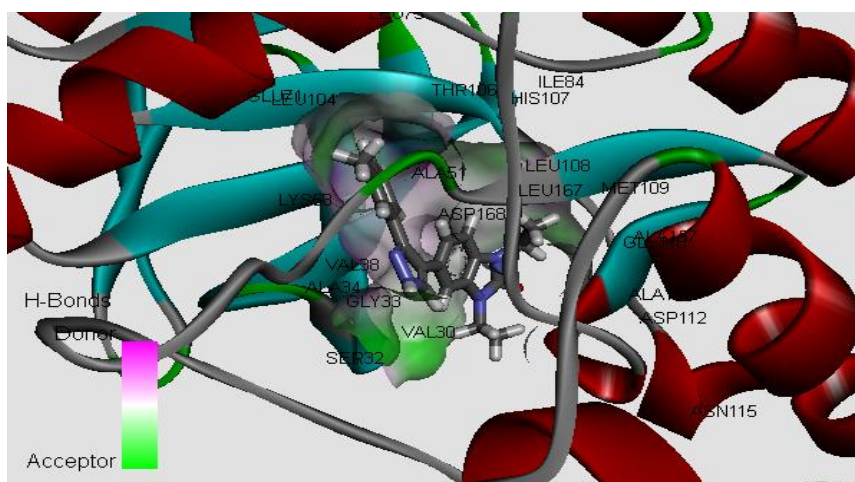


Figure 11: Binding mode of compound **34** with P38 alpha. The enzyme is shown as surface; while compound **34** docked structures are shown as ball and sticks. This figure was made using Discovery Studio 3.5.

4. Conclusion

In this paper, we have employed 3D-QSAR and docking techniques to explore the structure-activity relationship of a series of 42 benzimidazolone derivatives as p38 kinase inhibitors. The MLR and NN methods were used to build significant statistically models. Validated by Cross-Validation method with LOO procedure, these models show good predictive, so that they could be used to predict new p38 kinase inhibitors. Molecular Docking of compounds 34 with p38 kinase inhibitors reveals important interactions by hydrogen links, electrostatic and VDW interactions. So, QSAR models could provide a reliable tool for reasonable synthesis of p38 kinase inhibitors in the future.

References

- [1] JeanMarie Lisnock , Andy Tebben , Betsy Frantz , Edward A. O'Neill , Gist Croft , Stephen J. O'Keefe , Bing Li , Candice Hacker , Stephen de Laszlo , Anthony Smith , Brian Libby , Nigel Liverton , Jeffrey Hermes , and Philip Lo Grasso, Molecular Basis for p38 Protein Kinase Inhibitor Specificity , Biochemistry, 1999, 38 : 3456–3456
- [2] Zhu Ming ,Wen-Juan Sun 1 , Yuan Li-Wang ,Qing Li ,Hong-Dan Yang ,Ze-Lin Duan ,Lin He, Wang Qu.,P38 participates in spermatogenesis and acrosome reaction prior to fertilization in Chinese mitten crab Eriocheir sinensis ,2015, 559:103–111
- [3] M. Krishna, H. Narang., The complexity of mitogen-activated protein kinases (MAPKs) made simple Cell. Mol. Life Sci, 2008, 65: 3525–3544
- [4] R.R. Jia, R.W. Gereau, M. Malcangioc, G.R. Strichartz,MAP kinase and pain Brain Res. Rev., 2009, 60 :135–148

- [5] J. Han, JD Lee, L. Bibbs, RJ Ulevitch., A MAP kinase targeted by endotoxin and hyperosmolarity in Science mammalian cells., 1994, 265: 808-811
- [6] Yilong Fu, Andy Yip, Peck Gee Seah, Francesca Blasco, Pei-Yong Shi, , Maxime Herve ,Modulation of inflammation and pathology during dengue virus infection by p38 MAPK inhibitor SB203580, Antiviral Research, 2014, 110: 151–157
- [7] Koichi Hasumi ,Shuichiro Sato ,Takahisa Saito ,Jun-Kato ya ,Kazuhiko Shirota ,Juin Sato , Hiroyuki Suzuki ` Shuji Ohta , Design and syntheses of 5 - [(2-chloro-6-fluoro phenyl) -acetyl amino] -3- (4-fluorophenyl) -4- (4-pyrimidinyl) isoxazole (AKP-001), a novel inhibitor of p38 MAP kinase with reduced side effects based on the concept of antedrug, Bioorganic and Medicinal Chemistry 2014 ,22 : 4162-4176.
- [8] Mark A. Dombroski, Michael A. Letavic,y Kim F. McClure, John T. Barberia, Thomas J. Carty, Santo R. Cortina, Csilla Csiki, Alan J. Dipesa, Nancy C. Elliott, Christopher A. Gabel, Crystal K. Jordan, Jeff M. Labasi, William H. Martin, Kevin M. Peese, Ingrid A. Stock, Linne Svensson, Francis J. Sweeney and Chul H. Yu., Benzimidazolone P₃₈ inhibitors, Bioorganic and Medicinal Chemistry Letters , 2004, 14 :919–923
- [9] Gilberto M. Sperandio da Silva ,Carlos M. Sant'Anna ,Eliezer J. Barreiro ,A novel 3D-QSAR comparative molecular field analysis (CoMFA) model of imidazole and quinazolinone functionalized p38 MAP kinase inhibitors , Bioorganic & Medicinal Chemistry, 2004, 12: 3159-3166
- [10] M.J. Frisch, G.W. Trucks, H.B. Schlegel, G.E. Scuseria, M.A. Robb, J.R. Cheeseman, J.J. A. Montgomery, T. Vreven, K.N. Kudin, J.C. Burant, J.M. Millam, S.S. Iyengar, J. Tomasi, V. Barone, B. Mennucci, M. Cossi, G. Scalmani, N. Rega, G.A. Petersson, H. Nakatsuji, M. Hada, M. Ehara, K. Toyota, R. Fukuda, J. Hasegawa, M. Ishida, T. Nakajima, Y. Honda, O. Kitao, H. Nakai, M. Klene, X. Li, J.E. Knox, H.P. Hratchian, J.B. Cross, V. Bakken, C. Adamo, J. Jaramillo, R. Gomperts, R.E. Stratmann, O. Yazyev, A.J. Austin, R. Cammi, C. Pomelli, J.W. Ochterski, P.Y. Ayala, K. Morokuma, G.A. Voth, P. Salvador, J.J. Dannenberg, V.G. Zakrzewski, S. Dapprich, A.D. Daniels, M.C. Strain, O. Farkas, D.K. Malick, A.D. Rabuck, K. Raghavachari, J.B. Foresman, J.V. Ortiz, Q. Cui, A.G. Baboul, S. Clifford, J. Cioslowski, B.B. Stefanov, G. Liu, A. Liashenko, P. Piskorz, I. Komaromi, R.L. Martin, D.J. Fox, T. Keith, M.A. Al-Laham, C.Y. Peng, A. Nanayakkara, M. Challacombe, P.M.W. Gill, B. Johnson, W. Chen, M.W. Wong, C. Gonzalez, J.A. Pople, Gaussian 03, Revision C.02, Gaussian, Inc., Wallingford CT, 2004.
- [11] R.G. Parr, L.v. Szentpaly, S. Liu, Electrophilicity index, Journal of the American Chemical Society 1999, 121: 1922–1924.
- [12] R.G. Parr, R.G. Pearson, Absolute hardness: companion parameter to absolute electronegativity, Journal of the American Chemical Society, 1983 ,105:7512–7516.
- [13] R.G. Parr, R.A. Donnelly, M. Levy, W.E. Palke, Electronegativity: the density functional viewpoint, Journal of Chemical Physics 1978, 68:3801–3807.
- [14] Schmidheiny, Kurt.; Universität Basel. The Multiple Linear Regression Model. 2015.
- [15] C.Nantasenamat, C. Isarankura-Na-Ayudhya, N. Tansila, T. Naenna, V. Prachayasittikul, Prediction of GFP spectral properties using artificial neural network, Journal of Computational Chemistry, 2008, 28 :1275–1289.
- [16] Elhallaoui, M. Modélisation moléculaire et étude QSAR d'antagonistes non compétitifs du récepteur NMDA par les méthodes statistiques et le réseau de neurones (Doctoral thesis) Fez (2003).

- [17] Mbarki, S.; El Hallaoui, M. 3D-QSAR models to predict antimoebic activities of the cyclised pyrazolines and 2-(quinolin-8-yloxy) acetohydrazones. *Research Journal of Pharmaceutical, Biological and Chemical Sciences* 2014, 5:73-83.
- [18] MRABTI ,N.N.; Dguigui ,K.; El Hallaoui ,M. QSAR Studies of Inhibitory Properties of 2-Substituant -1H-Benzimidazole-4-Carboxamide derivatives against enteroviruses. *International Journal of Innovative Research in Science, Engineering and Technology* 2014,3:201-213.
- [19] Kharb, M.; Jat, R.K., Parjapati, G.; Gupta, A. Introduction to molecular docking software technique in medicinal chemistry. *International Journal of Drug Research and Technology* 2012,2:189-197.
- [20]<https://wiki.csiro.au/display/ASC/Install+Accelrys+Discovery+Studio+3.5+on+Windows>.
- [21] Hamed I. Ali, Keiichiro Tomita, Eiichi Akaho, Hiroto Kambara, Shinji Miura, Hiroyuki Hayakawa, Noriyuki Ashida, Yutaka Kawashima, Takehiro Yamagishi, Hisao Ikeya, Fumio Yoneda, Tomohisa Nagamatsu, Antitumor studies. Part 1: Design, synthesis, antitumor activity, and AutoDock study of 2-deoxo-2-phenyl-5-deazaflavins and 2-deoxo-2-phenylflavin-5-oxides as a new class of antitumor agents, *Bioorganic and Medicinal Chemistry*, 2007, 15: 242-256
- [22] ACD/Labs Extension for ChemDraw Version 9.0 for Microsoft Windows User's Guide.